Long-range coupling and scalable architecture for superconducting flux qubits

Austin G. Fowler,[1] William F. Thompson,[1] Zhizhong Yan,[1] Ashley M. Stephens,[2] B. L. T. Plourde,[3] and Frank K. Wilhelm[1]
[1]*Institute for Quantum Computing, University of Waterloo, Waterloo, Ontario, Canada N2L 3G1*
[2]*Centre for Quantum Computer Technology, University of Melbourne, Victoria 3010, Australia*
[3]*Department of Physics, Syracuse University, Syracuse, New York 13244, USA*
(Received 20 April 2007; revised manuscript received 27 August 2007; published 12 November 2007)

Constructing a fault-tolerant quantum computer is a daunting task. Given any design, it is possible to determine the maximum error rate of each type of component that can be tolerated while still permitting arbitrarily large-scale quantum computation. It is an underappreciated fact that including an appropriately designed mechanism enabling long-range qubit coupling or transport substantially increases the maximum tolerable error rates of all components. With this thought in mind, we take the superconducting flux qubit coupling mechanism described by Plourde *et al.* [Phys. Rev. B **70**, 140501(R) (2004)] and extend it to allow approximately 500 MHz coupling of square flux qubits, 50 μm a side, at a distance of up to several millimeters. This mechanism is then used as the basis of two scalable architectures for flux qubits taking into account cross-talk and fault-tolerant considerations such as permitting a universal set of logical gates, parallelism, measurement and initialization, and data mobility.

DOI: 10.1103/PhysRevB.76.174507 PACS number(s): 03.67.Lx

I. INTRODUCTION

The field of quantum computation is largely concerned with the manipulation of two state quantum systems called qubits. Unlike the bits in today's computers which can be either 0 or 1, qubits can be placed in arbitrary superpositions $\alpha|0\rangle+\beta|1\rangle$ and entangled with each other. For a complete review of the basic properties of qubits and quantum information, see Ref. 2. The attraction of quantum computation lies in the existence of quantum algorithms that are in some cases exponentially faster than their best known classical equivalents. Most famous are Shor's factoring algorithm[3] and Grover's search algorithm.[4] There has also been extensive work on using a quantum computer to simulate quantum physics,[5–9] an ongoing exploration of adiabatic algorithms,[10–12] plus the discovery of quantum algorithms for differential equations,[13] finding eigenvalues,[14,15] numerical integration,[16] and various problems in group theory[17–19] and knot theory.[20,21]

Quantum systems suffer from decoherence, meaning their state rapidly becomes unknowable through unwanted interaction with the environment. Flux qubit decoherence times of up to a few microseconds have been demonstrated[22] versus single-qubit gate times of the order of 10 ns, and likely initial two-qubit gate times of the order of a few tens of nanoseconds.[1,23,24] To perform long quantum computations, quantum error correction will be required.[25–27] It has been shown that provided the totality of decoherence and control errors is below some nonzero threshold, and given an arbitrarily long time and an arbitrary large number of qubits, an arbitrarily long and large quantum computation can be performed.[28] Despite being well known in certain circles, the broader quantum computing community has not yet sufficiently come to terms with the fact that long-range interactions permit much higher levels of decoherence and control error to be tolerated. With unlimited range interactions and extremely large numbers of qubits, the threshold error rate has been shown to be of the order of 10^{-2}.[29] With fewer qubits but still unlimited range interactions, the threshold is reduced to between 10^{-3} and 10^{-4}.[30] A two-dimensional lattice of qubits interacting with their nearest neighbors only has been devised with an approximate threshold of 10^{-5}.[31] The full analysis of an infinite double line of qubits with nearest neighbor interactions has been performed, yielding a lower bound to the threshold of 1.96×10^{-6}.[32] Work on an infinite single line of qubits with nearest neighbor interactions is in progress, and the threshold is expected to be of the order of 10^{-8}.[33]

Despite the extremely low expected threshold of linear nearest neighbor architectures, a great deal of theoretical work has been devoted to the design of such architectures using a variety of physical systems.[34–44] This is reasonable in the context of providing an experimental starting point, but we believe the time has come to expect at least a theoretical proposal for how long-range interactions or long-distance qubit transport might be performed. Without this, it is extremely difficult to argue the long-term viability of a given system. Furthermore, any proposed method of interaction or transport must be capable of being performed in parallel on a number of pairs of qubits that grow linearly with the size of the computer to permit the simultaneous application of error correction to a constant fraction of the logical qubits in the computer. In contrast, a quantum computer based around a single, global, serial interaction or transport mechanism, such as a single resonator shared by all qubits in the computer,[45] cannot simultaneously apply quantum error correction to multiple logical qubits. Such a quantum computer could, at best, apply quantum error correction to each logical qubit in turn. As the number of logical qubits increases and the amount of time between applications of error correction to a given logical qubit increases, more errors accumulate and the probability of successful error correction decreases. Beyond a certain amount of time between error correction applications, it is overwhelmingly likely that every physical qubit comprising a given logical qubit will have suffered an error, meaning no amount of quantum error correction will successfully recover the original logical state. Consequently,

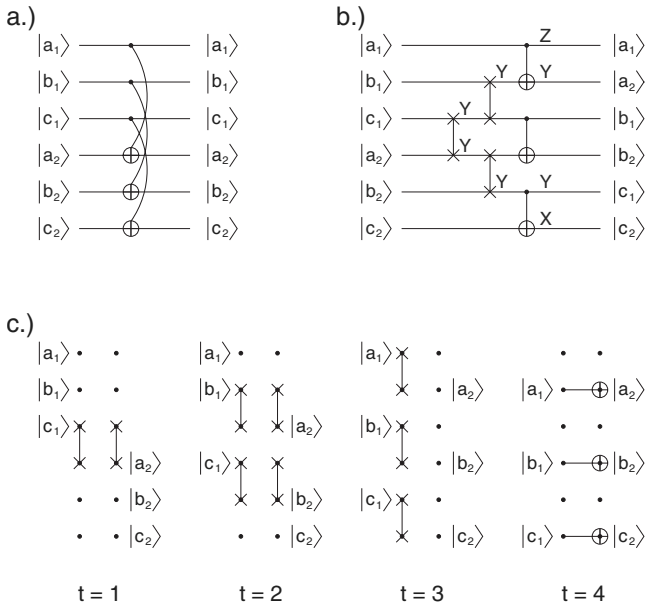

FIG. 1. (a) Nonlocal transversal interaction. (b) Naive linear nearest neighbor transversal interaction showing the propagation of errors resulting from the failure of a single swap gate, leading to two errors in both logical qubits. (c) The first four time steps of a bilinear fault-tolerant transversal interaction between two sets of three physical qubits. The remaining three steps are the time reverse of the first three steps.

any quantum computer based around a single, global, serial interaction or transport mechanism is not scalable in the sense that it could never perform an arbitrarily large quantum computation.

The purpose of this paper is to present a long-range coupling mechanism for superconducting flux qubits that can be used to couple many pairs of qubits together in parallel in a manner suited to the construction of an arbitrarily large fault-tolerant quantum computer. In Sec. II, we review the coupling mechanism of Refs. 1 and 23, and extend it to allow long-range coupling in Sec. III. In Sec. IV, we firstly describe a simple, yet scalable, flux qubit architecture based on this interaction, but not taking full advantage of it, then a more complicated architecture with a better threshold error rate, though much more difficult to build. Finally, Sec. V concludes with a summary of results and a description of further work.

II. COUPLING FLUX QUBITS

Before discussing our coupling mechanism, a few words elaborating exactly why long-range interactions are advantageous are in order. Essentially, the problem lies in the need to perform transversal multiple logical qubit gates, as shown in Fig. 1(a). If long-range interactions are available, two logical qubits each comprised of n physical qubits can be transversely interacted in a single time step using n gates. If we now try to do the same thing on a linear nearest neighbor architecture using swap gates prior to the necessary gates to perform the transversal interaction, we immediately run into a serious problem. A single swap gate failure can lead to two errors in a single logical qubit as shown in Fig. 1(b). Under normal circumstances, two or more errors in a single logical qubit are not correctable. A solution to this dilemma that avoids the need to resort to a multiple error correcting code is shown in Fig. 1(c), where a second line of placeholder qubits has been added. Now swap gates never simultaneously touch two qubits that are both part of logical qubits. Note that the first three steps of Fig. 1(c) need to be repeated, time reversed, to return the qubits to their original configuration. We can now see that to interact two n-qubit logical qubits transversely and fault tolerantly using only nearest neighbor interactions, using the scheme described, we need $4n$ qubits, $2n^2+n$ gates, and $2n+1$ time steps with $2n^2$ locations where data qubits are left idle. For all of this additional machinery to result in a circuit with the same reliability as the nonlocal case, every individual component must be significantly more reliable. This is the origin of the lower thresholds quoted in the Introduction for ever more constrained architectures.

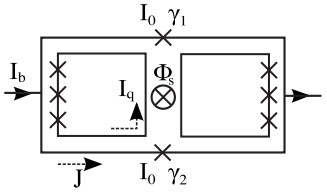

FIG. 2. Coupling scheme as proposed in Ref. 1, including circuit symbols and orientations.

With the above motivation in mind, we proceed to the discussion of coupling superconducting flux qubits. Coherent oscillations of the state of a superconducting flux qubit were first demonstrated at Delft in 2003.[46] A number of other institutions are also developing flux qubit technology, including Berkeley,[23] NEC,[47,48,58] RIKEN,[49,50] NTT,[51] and IPHT.[52] A flux qubit is essentially a superconducting ring interrupted by typically three Josephson junctions with clockwise and anticlockwise persistent currents forming the basis of an effective two level quantum system. For an up-to-date review of superconducting qubit theory in general, including flux qubits, see Ref. 53.

The coupling scheme as proposed in Ref. 1 is shown, somewhat simplified, in Fig. 2. Let K_0 denote the strength of the direct inductive coupling between the qubits, M_{qq} the mutual inductance of the qubits, and $|I_q|$ the magnitude of the qubit circulating current. Note that in Ref. 1, the algebraic analysis was done with potentially different current magnitudes $|I_q^{(1)}|$ and $|I_q^{(2)}|$, but the numerical analysis was done with $|I_q^{(1)}|=|I_q^{(2)}|=0.48$ μA. The above quantities are related by $K_0=2M_{qq}I_q^2$. Let K_s denote the strength of the coupling mediated by the superconducting quantum interference device (SQUID), M_{qs} the mutual inductance between either of the qubits and the SQUID, J the circulating current in the SQUID, Φ_s the flux through the SQUID, and I_b the SQUID bias current. These are related by

$$K_s = 2M_{qs}^2 I_q^2 \left(\frac{\partial J}{\partial \Phi_s}\right)_{I_b}. \tag{1}$$

In the slowly varying and high resistance limit of the junctions, we can write

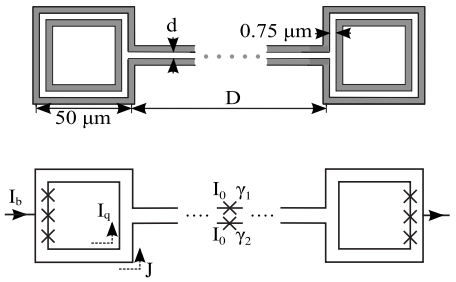

FIG. 3. Extending coupling scheme, including circuit symbols, orientations, and dimensions. All wires are 0.75 μm wide and 0.1 μm thick.

$$I_b = I_0 \sin \gamma_1 + I_0 \sin \gamma_2, \tag{2}$$

$$2J = I_0 \sin \gamma_2 - I_0 \sin \gamma_1, \tag{3}$$

where γ_1 and γ_2 are the phase drops across the SQUID Josephson junctions. This can be written as

$$I_b = 2I_0 \sin \bar{\gamma} \cos \Delta\gamma, \tag{4}$$

$$J = I_0 \sin \Delta\gamma \cos \bar{\gamma}, \tag{5}$$

where $\Delta\gamma = \frac{\gamma_2 - \gamma_1}{2}$ and $\bar{\gamma} = \frac{\gamma_1 + \gamma_2}{2}$. These equations are constrained by

$$\Delta\gamma = \frac{\pi}{\Phi_0}(\Phi_s - LdJ), \tag{6}$$

where L is the inductance of the coupler and Φ_s is nominally set to $\Phi_s = 0.45\Phi_0$ to maximize the response of J to variations in Φ_s. Taking the partial derivative of Eqs. (4)–(6) with respect to Φ_s, we obtain

$$\frac{\partial I_b}{\partial \Phi_s} = 0 = 2I_0 \frac{\partial}{\partial \Phi_s}(\cos \Delta\gamma \sin \bar{\gamma}), \tag{7}$$

$$\frac{\partial J}{\partial \Phi_s} = I_0 \left[-\frac{\partial \bar{\gamma}}{\partial \Phi_s} \sin \bar{\gamma} \sin \Delta\gamma + \frac{\partial \Delta\gamma}{\partial \Phi_s} \cos \bar{\gamma} \cos \Delta\gamma \right], \tag{8}$$

$$\frac{\partial \Delta\gamma}{\partial \Phi_s} = \frac{\pi}{\Phi_0}\left(1 - L\frac{\partial J}{\partial \Phi_s}\right). \tag{9}$$

Using these equations, we can derive the expression

$$\left(\frac{\partial J}{\partial \Phi_s}\right)_{I_b} = \frac{1}{2L_j} \frac{1 - \tan^2 \bar{\gamma} \tan^2 \Delta\gamma}{1 + \frac{L}{2L_j}(1 - \tan^2 \bar{\gamma} \tan^2 \Delta\gamma)}, \tag{10}$$

where $L_j = \Phi_0 / 2\pi I_0 \cos \Delta\gamma \cos \bar{\gamma}$ is the Josephson inductance. This expression characterizes the tunable nature of the coupling scheme.

III. LONG-RANGE COUPLING

We propose modifying the coupler as shown in Fig. 3. All dimensions are typical of the Berkeley group.[23] This design results in decreased mutual inductance between the qubits, increased mutual inductance between the qubits and the coupler, increased self-inductance of the coupler, and significant capacitance structurally incorporated into the coupler. All of these effects will be investigated as well as the resultant impact on the coupling strength.

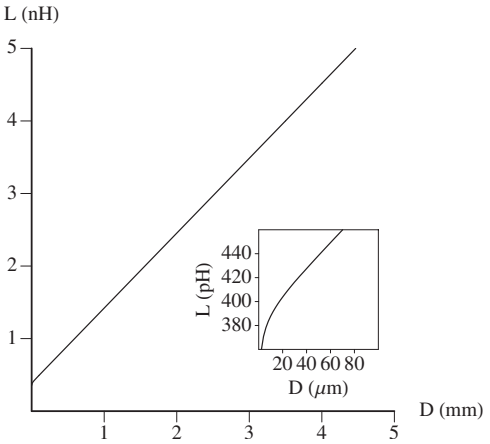

FIG. 4. The self-inductance of the coupler as a function of the length of the coupler.

Before discussing coupling strengths, we need to determine the various inductances of the new system. Figure 4 shows the self-inductance of the coupler versus coupler length D for coupler width $d = 1.5$ μm, generated using FASTHENRY, assuming superconducting aluminum wires with a penetration depth of 49 nm.[54] The inset shows the short length behavior. For all lengths of interest, the coupler self-inductance is approximately given by $(356 + 0.863D/\mu\text{m})$ pH. A small value of d is desirable to minimize L at a given length and, as we shall see, maximize the coupling strength. However, this also introduces a large capacitance, with consequences to be discussed at the end of this section. The mutual inductance of each qubit with the coupler was found to be 75 pH.

We are now in a position to calculate the coupler mediated coupling strength K_s for zero bias current, done numerically for two different critical currents $I_0 = 0.48$ and 0.16 μA, and shown in Fig. 5. Note the existence of optimum lengths, 700 and 2500 μm, respectively, a consequence of the cosine terms in L_j. The coupling strength due to the mutual inductance of the qubits is shown in Fig. 6. Note that to neglect the

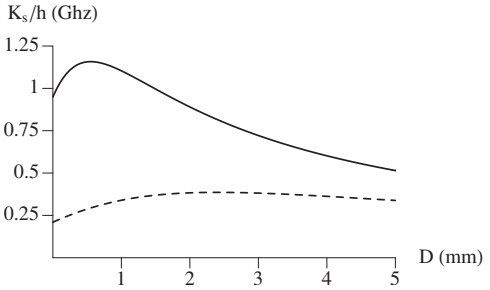

FIG. 5. The coupling strength at zero bias current ($\Phi_s = 0.45\Phi_0$) without mutual qubit interaction versus the length of the coupler for $I_0 = 0.48$ μA (solid) and $I_0 = 0.16$ μA (dashed).

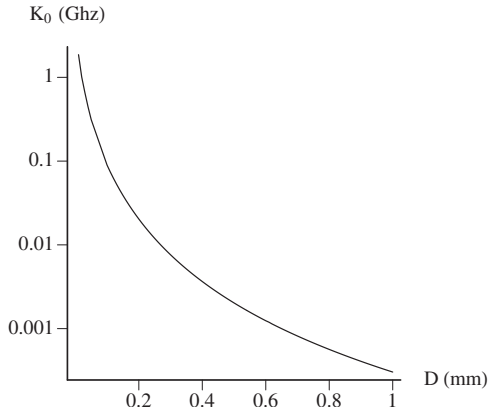

FIG. 6. The strength of the direct qubit-qubit interaction due to mutual inductive coupling as a function of the length of the coupler, and thus, qubit separation.

direct mutual coupling, it is necessary for the qubits to be separated by approximately 650 μm, corresponding to a coupling strength approximately 3 orders of magnitude less than that induced by a coupler of length 650 μm. Its consequences in architecture design will be discussed in Sec. IV.

The coupling strength can be reduced to zero by sufficiently increasing the bias current. It is desirable to ensure that the necessary increase is as small as possible, as the presence of a bias current, particularly one close to the critical current, is a significant source of decoherence.[1,47,55] Figure 7 shows the coupling strength versus bias current for a selection of four coupler lengths. This figure uses the critical current I_0=0.48 μA from Ref. 1. Clearly, particularly for long lengths, the bias current required to achieve zero coupling strength is too close to the critical current. This problem can be circumvented by reducing the critical current of the junctions to I_0=0.16 μA, resulting in Fig. 8. Reducing the critical current reduces the zero bias coupling strength, lowering the ratio I_b/I_c required to achieve zero coupling strength.

In principle, Fig. 8 is promising, both in terms of coupling strength and coupling length. However, the effect of the capacitance of the coupler must be determined. As a starting point, consider a single flux qubit initially prepared in a clockwise current state. Left alone, this qubit will oscillate between clockwise and anticlockwise current states at its tunneling frequency, which is typically of the order of a few

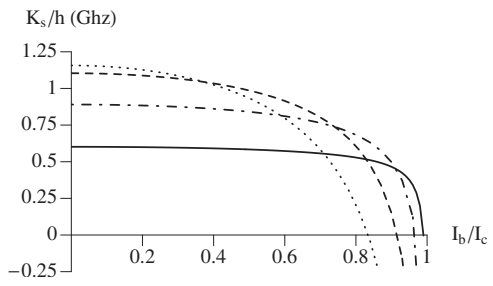

FIG. 7. The coupling strength as a function of the bias current with Φ_s=0.45Φ_0 and I_c=$I_c(\Phi_s)$, using Josephson junction critical currents of I_0=0.48 μA. D=500 μm (dotted), D=1000 μm (dashed), D=2000 μm (dash-dotted), and D=4000 μm (solid).

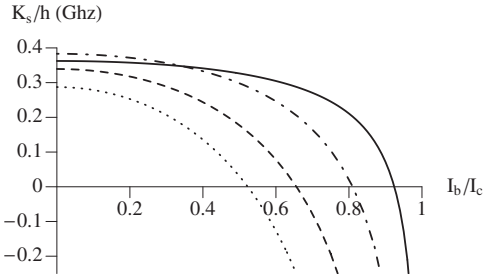

FIG. 8. The coupling strength as a function of the bias current with Φ_s=0.45Φ_0 and I_c=$I_c(\Phi_s)$, using Josephson junction critical currents of I_0=0.16 μA. D=500 μm (dotted), D=1000 μm (dashed), D=2000 μm (dash-dotted), and D=4000 μm (solid).

gigahertz in current devices. As seen by the coupler, by virtue of their mutual inductance, such a qubit plays the role of an alternating current source. Considering the coupler in isolation now, we wish to check that an alternating current source at one end of the coupler with amplitude A generates an alternating current of amplitude as close to A as possible at the other end. Using a lumped circuit model and discretizing the capacitive section of the coupler, deviation from perfect transmission of the order of 1% was found. This is low enough to give us confidence that the fundamental concept of the extended coupler is sound, but high enough that achieving high fidelity gates will require a closer examination of the physics of the system.[56] We have also begun simulations of the complete system including silicon substrate using the commercial package HFSS. The results of these simulations and capacitive and radiative effects, in general, will be discussed in detail in a separate publication.

IV. ARCHITECTURES

In quantum computing literature, the word "scalable" is, regrettably, frequently used rather loosely, and sometimes inaccurately. Ideally, as a minimum, it should only be claimed that an architecture is scalable if, in principle, an arbitrarily large number of qubits can be implemented, the number of quantum gates and measurements that can be executed simultaneously grows linearly with the number of qubits, and the physics of any one quantum gate or measurement does not depend on the total number of qubits. A simple example of such an architecture making use of the coupler described in this paper is shown, not drawn to scale, in Fig. 9(a). This figure shows eight qubits with three couplers around each qubit, each electrically isolated from the others, which is feasible with current layering technology. These have been drawn one on top of another. Note that one qubit of each pair of qubits in each coupler is more weakly coupled to the coupler following Ref. 23; this is indicated by the increased spacing in the figure between the qubit and the coupler. This enables readout of both qubits simultaneously using one coupler via the resonant readout scheme of Ref. 57. Also shown in the figure are current bias lines for each coupler with, for example, the group of three lines entering the couplers surrounding the top left qubit representing the current bias lines for the left, downward, and right leading couplers, respec-

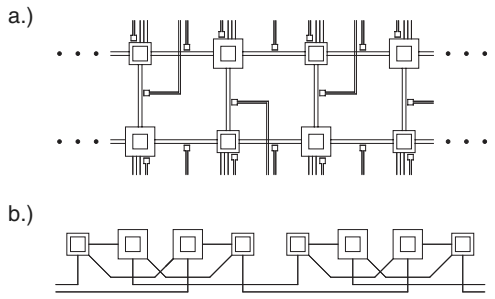

FIG. 9. (a) Simple scalable bilinear flux qubit architecture including flux lines for each coupler and qubit. As drawn, the architecture requires three layers of metal corresponding to the three couplers around each qubit. See Sec. IV for a full description of the various components of the figure. (b) Topologically identical array used as the basis of Fig. 11.

tively. Lastly, both the qubits and the couplers need independent flux bias lines, represented by small current loops near each of the qubits and each center of the couplers. These flux bias lines keep both the qubits and couplers at their optimal working points, and provide the pulses for single-qubit gates.

Given the large potential length of each coupler, cross-talk can be neglected, and with only a small number of control lines leading to external circuitry per pair of qubits, given a sufficiently large fridge, many qubits can be accommodated. The details of how many qubits and how to include the necessary control lines and classical control machinery shall be left for a future publication. Two lines of qubits have been incorporated in the design to permit simpler error correction, resulting in a threshold two-qubit gate error rate for arbitrarily large fault-tolerant quantum computation of 1.96×10^{-6} as described in Ref. 32. Note that to use this architecture in practice, this implies the need for two-qubit gates operating with an error rate of 10^{-7} or less, far below what is achievable in most solid-state systems given the current ratios of decoherence times to gate times.

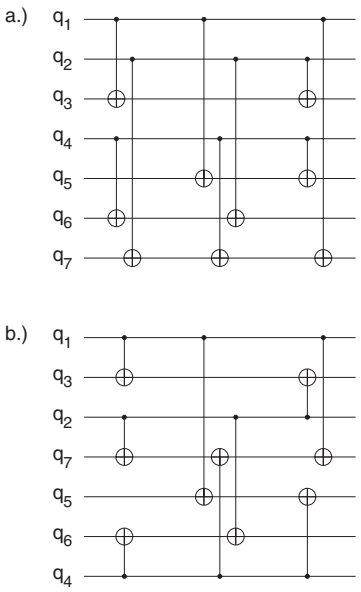

FIG. 10. To reduce the need for long-range interactions, the circuit (a) taken from Ref. 27, which encodes and decodes a logical zero, was modified as shown in (b) by swapping two pairs of qubits.

Of course, the architecture of Fig. 9(a) does not take full advantage of the potential length of the coupler. As discussed earlier, to ensure relatively low cross-talk, from Fig. 4, qubits need to be spaced approximately 650 μm apart. This still gives us enough space to firstly stretch the architecture of Fig. 9(a) into a single line as shown in Fig. 9(b), then duplicate this line seven times to permit an additional layer of the seven-qubit Steane code to be used. Referring to Fig. 11, these duplicated qubits correspond to the bottom seven qubits in each group of 21. The middle row of qubits in each group of 21 corresponds to ancilla qubits used during error correction according to the scheme described in Ref. 27, with

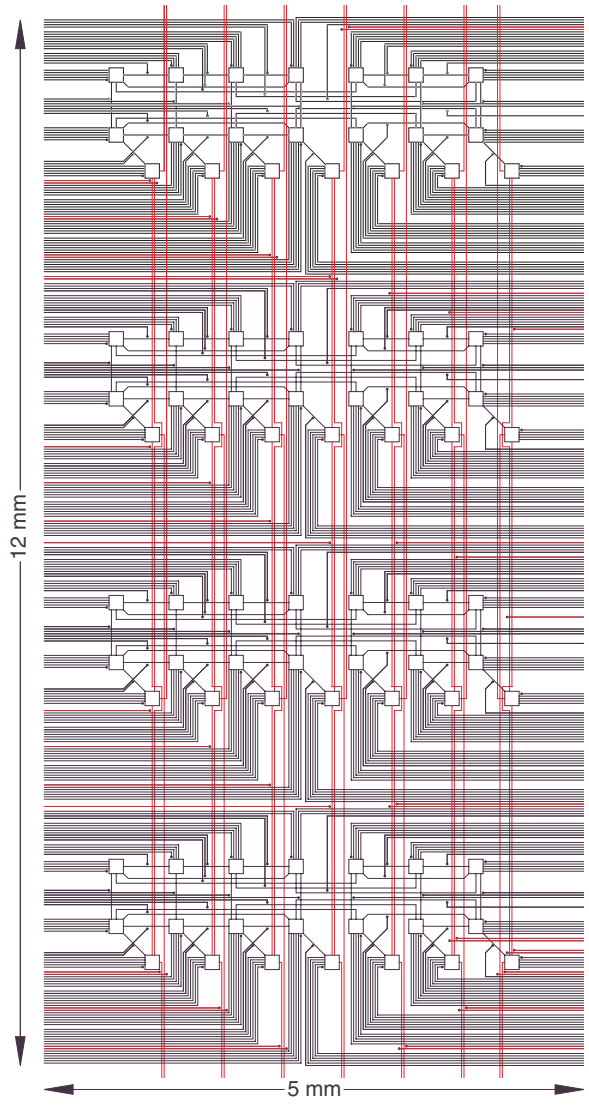

FIG. 11. (Color online) A complete architecture for a flux qubit quantum computer. Squares represent flux qubits, lines connecting squares represent SQUID couplers, lines running away from each square represent squid bias current lines, and small dots with lines running away from them represent qubit and SQUID flux bias lines. The size of the flux qubits has been exaggerated for clarity. Red lines represent the SQUIDs and flux bias lines for the second and higher levels of error correction and logical gates.

slight modifications to reduce the range of the necessary interactions as shown in Fig. 10. The top row of qubits in each group of 21 corresponds to ancilla qubits only used during the implementation of the fault-tolerant T gate, or $\pi/8$ gate, as it is also known, which is required to ensure that the computer can perform a universal set of fault-tolerant gates. A complete description of the circuitry of this gate can be found in Ref. 32. Note that, even with all the additional control lines, the architecture requires just one wire per approximately 40 μm per side.

The network of qubits and couplers shown in Fig. 11 enables the most efficient known nonlocal error correction scheme and fault-tolerant gates to be implemented at the lowest level. All higher levels make use of the circuitry devised for the bilinear architecture. When the threshold two-qubit error rate of this more complicated architecture was calculated, using the mathematical tools described in Ref. 32, the disappointingly low result of 6.25×10^{-6} was obtained—just over a factor of 3 better than the bilinear array. In short, the dominant nearest neighbor behavior of the large-scale architecture is not overcome by a single layer of nonlocal error correction and gates.

V. CONCLUSION

We have described in detail a nonlocal method of coupling pairs of flux qubits and shown that it is suited to the construction of complex, scalable quantum computer architectures as shown in Fig. 11. By virtue of the fact that flux qubits do not require large quantities of classical control circuitry on a chip, there are no obvious lithographic or heat dissipation barriers to the construction of such an architecture. The primary concern, as with all superconducting quantum technology, is decoherence. In the near future, we wish to look at other superconducting qubits and coupling schemes with the aim of removing all known sources of decoherence from the design. For example, in Ref. 47, a method of coupling flux qubits tunably is described that does not resort to a nonzero SQUID bias current. Furthermore, the need for large qubit separations to minimize cross-talk could, in principle, be alleviated by enclosing each qubit in a micrometer scale Meissner cage. Devising a more practical method of achieving higher qubit densities would greatly increase the utility of the proposed coupling scheme. Finally, with or without higher qubit densities, additional architecture design work is required to try to raise the threshold further, possibly by attempting to incorporate two layers of nonlocal error correction into the design.

ACKNOWLEDGMENTS

A.G.F and F.K.W would like to thank S. Oh for helpful discussions. This work was supported by a NSERC Discovery Grant and the European Union through EuroSQIP.

[1] B. L. T. Plourde *et al.*, Phys. Rev. B **70**, 140501(R) (2004).
[2] M. A. Nielson and I. L. Chuang, *Quantum Computation and Quantum Information* (Cambridge University Press, Cambridge, England, 2000).
[3] P. W. Shor, Proceedings of the 35th Annual Symposium on Foundations of Computer Science, 1994 (unpublished), pp. 124–134.
[4] L. K. Grover, Proceedings of the 28th Annual ACM Symposium on the Theory of Computing, May 1996 (unpublished), pp. 212–219.
[5] R. P. Feynman, Int. J. Theor. Phys. **21**, 467 (1982).
[6] S. Lloyd, Science **273**, 1073 (1996).
[7] B. M. Boghosian and W. Taylor, Physica D **120**, 30 (1998).
[8] A. T. Sornborger and E. D. Stewart, Phys. Rev. A **60**, 1956 (1999).
[9] T. Byrnes and Y. Yamamoto, Phys. Rev. A **73**, 022328 (2006).
[10] E. Farhi, J. Goldstone, S. Gutmann, J. Lapan, A. Lundgren, and D. Preda, Science **292**, 472 (2001).
[11] A. M. Childs, E. Farhi, J. Goldstone, and S. Gutmann, Quantum Inf. Comput. **2**, 181 (2002).
[12] M. C. Banuls, R. Orus, J. I. Latorre, A. Perez, and P. Ruiz-Femenia, Phys. Rev. A **73**, 022344 (2006).
[13] T. Szkopek, V. Roychowdhury, and E. Yablonovitch, Phys. Rev. A **72**, 062318 (2004).
[14] D. S. Abrams and S. Lloyd, Phys. Rev. Lett. **83**, 5162 (1999).
[15] P. Jaksch and A. Papageorgiou, Phys. Rev. Lett. **91**, 257902 (2003).
[16] D. S. Abrams and C. P. Williams, arXiv:quant-ph/9908083 (unpublished).
[17] A. Y. Kitaev, Technical Report No. TR96-003, 1996 (unpublished).
[18] M. Mosca and A. Ekert, Lect. Notes Comput. Sci. **1509**, 174 (1999).
[19] S. A. Fenner and Y. Zhang, Proceedings of the Ninth IC-EATCS Italian Conference on Theoretical Computer Science, 2005 (unpublished), pp. 215–227.
[20] V. Subramaniam and P. Ramadevi, arXiv:quant-ph/0210095 (unpublished).
[21] P. Wocjan and J. Yard, arXiv:quant-ph/0603069 (unpublished).
[22] P. Bertet, I. Chiorescu, G. Burkard, K. Semba, C. J. P. M. Harmans, D. P. DiVincenzo, and J. E. Mooij, Phys. Rev. Lett. **95**, 257002 (2005).
[23] T. Hime, P. A. Reichardt, B. L. T. Plourde, T. L. Robertson, C.-E. Wu, A. V. Ustinov, and J. Clarke, Science **314**, 1427 (2006).
[24] S. H. W. van der Ploeg, A. Izmalkov, A. M. van den Brink, U. Hübner, M. Grajcar, E. Il'ichev, H.-G. Meyer, and A. M. Zagoskin, Phys. Rev. Lett. **98**, 057004 (2007).
[25] A. R. Calderbank and P. W. Shor, Phys. Rev. A **54**, 1098 (1996).
[26] A. M. Steane, Proc. R. Soc. London, Ser. A **425**, 2551 (1996).
[27] D. P. DiVincenzo and P. Aliferis, Phys. Rev. Lett. **98**, 020501 (2007).
[28] E. Knill, R. Laflamme, and W. H. Zurek, Los Alamos National Laboratory, Technical Report No. LAUR-96-2199, 1996 (unpublished).
[29] E. Knill, arXiv:quant-ph/0410199 (unpublished).
[30] A. M. Steane, Phys. Rev. A **68**, 042322 (2003).
[31] K. M. Svore, D. DiVincenzo, and B. Terhal, Quantum Inf. Com-

put. **7**, 297 (2007).
[32] A. M. Stephens, A. G. Fowler, and L. C. L. Hollenberg, arXiv:quant-ph/0702201 (unpublished).
[33] A. M. Stephens, A. G. Fowler, and L. C. L. Hollenberg (unpublished).
[34] N.-J. Wu, M. Kamada, A. Natori, and H. Yasunaga, Jpn. J. Appl. Phys., Part 1 **39**, 4642 (2000).
[35] R. Vrijen, E. Yablonovitch, K. Wang, H. W. Jiang, A. Balandin, V. Roychowdhury, T. Mor, and D. DiVincenzo, Phys. Rev. A **62**, 012306 (2000).
[36] B. Golding and M. I. Dykman, arXiv:cond-mat/0309147 (unpublished).
[37] E. Novais and A. H. Castro Neto, Phys. Rev. A **69**, 062312 (2004).
[38] L. C. L. Hollenberg, A. S. Dzurak, C. Wellard, A. R. Hamilton, D. J. Reilly, G. J. Milburn, and R. G. Clark, Phys. Rev. B **69**, 113301 (2004).
[39] L. Tian and P. Zoller, Phys. Rev. A **68**, 042321 (2003).
[40] M. Friesen, P. Rugheimer, D. E. Savage, M. G. Lagally, D. W. van der Weide, R. Joynt, and M. A. Eriksson, Phys. Rev. B **67**, 121301(R) (2003).
[41] L. M. K. Vandersypen, R. Hanson, L. H. W. van Beveren, J. M. Elzerman, J. S. Greidanus, S. D. Franceschi, and L. P. Kouwenhoven, in *Quantum Computing and Quantum Bits in Mesoscopic Systems*, edited by A. J. Leggett, B. Ruggiero, and P. Silvestrini (Kluwer Academic, Dordrecht/Plenum, New York, 2003).
[42] P. Solinas, P. Zanardi, N. Zanghi, and F. Rossi, Phys. Rev. B **67**, 121307(R) (2003).
[43] V. V'yurkov and L. Y. Gorelik, J. Quantum Comput. Comput. **1**, 77 (2000).
[44] E. O. Kamenetskii and O. Voskoboynikov, in *Trends in Quantum Computing Research*, edited by Susan Shannon (Nova Science, New York, 2006).
[45] J. Q. You, J. S. Tsai, and F. Nori, Phys. Rev. Lett. **89**, 197902 (2002).
[46] I. Chiorescu, Y. Nakamura, C. J. P. M. Harmans, and J. E. Mooij, Science **299**, 1869 (2003).
[47] A. O. Niskanen, Y. Nakamura, and J.-S. Tsai, Phys. Rev. B **73**, 094506 (2006).
[48] A. O. Niskanen, K. Harrabi, F. Yoshihara, Y. Nakamura, and J.-S. Tsai, Phys. Rev. B **74**, 220503(R) (2006).
[49] Y.-X. Liu, L. F. Wei, J. S. Tsai, and F. Nori, Phys. Rev. Lett. **96**, 067003 (2006).
[50] M. Grajcar, Y.-X. Liu, F. Nori, and A. M. Zagoskin, Phys. Rev. B **74**, 172505 (2006).
[51] K. Kakuyanagi, T. Meno, S. Saito, H. Nakano, K. Semba, H. Takayanagi, F. Deppe, and A. Shnirman, Phys. Rev. Lett. **98**, 047004 (2007).
[52] M. Grajcar, A. Izmalkov, and E. Il'ichev, Phys. Rev. B **71**, 144501 (2005).
[53] M. R. Geller, E. J. Pritchett, A. T. Sornborger, and F. K. Wilhelm, in *Manipulating Quantum Coherence in Solid State Systems*, edited by M. E. Flatté and I. Tifrea (Springer, Dordrecht, 2007).
[54] T. E. Faber and A. B. Pippard, Proc. R. Soc. London, Ser. A **231**, 336 (1955).
[55] C. H. van der Wal, F. K. Wilhelm, C. J. P. M. Harmans, and J. E. Mooij, Eur. Phys. J. B **31**, 111 (2003).
[56] C. Hutter, A. Shnirman, Y. Makhlin, and G. Schön, Europhys. Lett. **74**, 1088 (2006).
[57] I. Serban, E. Solano, and F. K. Wilhelm, Phys. Rev. B **76**, 104510 (2007).
[58] A. O. Niskanen, K. Harrabi, F. Yoshihara, Y. Nakamura, S. Lloyd, and J. S. Tsai, Science **316**, 723 (2007).